Space-time dynamics of the vacuum's polarization charge density

A. T. Steinacher, J. Betke, S. Ahrens, Q. Su, and R. Grobe
Intense Laser Physics Theory Unit and Department of Physics, Illinois State University, Normal, Illinois 61790-4560, USA
(Received 6 March 2014; published 10 June 2014)

Using numerical solutions to the quantum-field theoretical Dirac equation, we study the space-time evolution of the vacuum's polarization charge and current densities induced by an external electric force in one spatial dimension. We discuss a simple analytical model that can predict the dynamics of the polarization dynamics for arbitrary external force configurations. We then study the corrections to these predictions when the external force becomes supercritical and real electron-positron pairs can be created. By coupling the Dirac equation to the Maxwell equations, we examine how the dynamics of the polarization density is affected, if we allow the corresponding induced charges to interact with each other.

DOI: 10.1103/PhysRevA.89.062106 PACS number(s): 12.20.Ds, 34.50.Rk, 03.65.−w

I. INTRODUCTION

The vacuum state plays a central role in quantum electrodynamics (QED). It is associated with the lowest-energy eigenstate in the interacting theory and is visualized as a state where none of the possible fermionic and bosonic states are excited, corresponding to the absence of any physical particles. Despite the absence of real particles, the vacuum has a rich structure, as revealed by many QED studies [1–7]. A fundamental property that characterizes any quantum theoretical state is the possibility of an induced charge displacement, i.e., the polarizability. In a pictorial sense, the vacuum can be thought of as an infinite reservoir of virtual photons, electrons and positrons that appear and disappear on short temporal and spatial scales. The vacuum polarization density can be modified due to the presence of a highly charged nucleus. If the nuclear charge is sufficiently large, the associated electric force can split the two fermions irreversibly, leading to the spontaneous pair creation from the vacuum as described in the pioneering work by Schwinger [8]. This breakdown process of the vacuum is predicted to emit positrons and captured electrons and establishes a new state in the supercritical field [3,9] called the charged vacuum. Due to its polarizability [10,11], the vacuum is sometimes compared to a dielectric medium. It has also been suggested that due to this polarization the vacuum is able to partially screen off any nucleus such that its effective charge, which is observed at distances farther than the electron's Compton wavelength, is typically smaller than the bare charge. This effect is also believed to contribute to a certain degree to the hydrogenic Lamb energy shift and is a main contributor to the corresponding energy shift of muonic helium [12,13]. This screening is interpreted as a consequence of the virtual pair production in the Coulombic background field of the charge.

The impact of the polarization has been examined on corrections to the binding energies of electrons or energies of positronic resonances in the static region, where the polarization is fully established. In this work we will examine the mechanisms leading to the occurrence and the space-time evolution of the polarization. If the polarization is based on electron and positron pairs, does their nonvanishing mass put a constraint on the maximum propagation speed of the polarization density? This question becomes more relevant as newly developed high-power laser sources will make direct experimental tests of the vacuum structure possible in this nonequilibrium regime [14].

The paper is structured as follows. In Sec. II we briefly review the framework of computational quantum-field theory that permits us to calculate the vacuum's charge and current densities for a one-dimensional system. We also show how to approximate the backreaction by coupling the Dirac equation to the Maxwell equations. In Sec. III we present the main finding of this work. In the absence of any real pair creation or backreaction the polarization density can be described by a remarkably simple wave equation, where the source term is directly proportional to the external charge distribution that was responsible for the external field. The proportionality constant (the vacuum's dynamical linear susceptibility) can be determined numerically. In Secs. IV and V we show how the polarization density is modified if the dynamics permits the creation of real electron-positron pairs or if the field's backreaction is taken into account. We finish with a brief summary and an outlook.

II. COMPUTATIONAL QUANTUM-FIELD THEORY IN ONE SPATIAL DIMENSION

We model the pair-creation process of the electron-positron pairs by the time-dependent Dirac Hamiltonian in one spatial dimension [15]:

$$H = c\sigma_1[p - q/cA(z,t)] + \sigma_3 mc^2 + qV(z,t), \qquad (2.1)$$

where $q = -1$ is the electronic charge, and σ_1 and σ_3 are the two Pauli matrices. In our numerical simulations below we use atomic and cgs units, where the four fundamental constants [amount of the electron charge $|q|$, the electron mass m, and Coulomb's and Planck's constants $1/(4\pi\varepsilon_0)$ and $\hbar$] are all unity by definition. As a result, the speed of light is $c = 137.036$ atomic units (a.u.).

The energy eigenstates of the force-free Hamiltonian (denoted by H_0) with positive energy $w_p \equiv [m^2c^4 + c^2p^2]^{1/2}$ and momentum p in the positive (up) energy continuum are denoted by $H_0|u;p\rangle = w_p|u;p\rangle$, whereas those in the negative (down) continuum are denoted by $H_0|d;p\rangle = -w_p|d;p\rangle$. Their spatial representation is

given by

$$\langle z|u;p\rangle \equiv W_p(u;z) = \eta[1, cp/(mc^2 + w_p)]\exp[ipz], \tag{2.2a}$$

$$\langle z|d;p\rangle \equiv W_p(d;z) = \eta[-cp/(mc^2 + w_p), 1]\exp[ipz], \tag{2.2b}$$

where $\eta \equiv (2\pi)^{-1/2}[1 + c^2p^2/(w_p + mc^2)^2]^{-1/2}$ denotes the normalization factor.

The vector and scalar potentials $A(z,t)$ and $V(z,t)$ in Eq. (2.1) represent the fields whose dynamical evolution is determined by the space-time–dependent charges and current densities $Q(z,t)$ and $J(z,t)$. In the Lorenz gauge $[\partial_z A = -\partial_{ct} V]$ the Maxwell equations read

$$\left(\partial_{ct}{}^2 - \partial_z{}^2\right)V(z,t) = 4\pi\, Q(z,t), \tag{2.3a}$$

$$\left(\partial_{ct}{}^2 - \partial_z{}^2\right)A(z,t) = 4\pi c^{-1} J(z,t). \tag{2.3b}$$

Below we analyze several physical scenarios. The induced electric charge and current densities due to the polarization of the vacuum, denoted by $\rho_{\rm pol}(z,t)$ and $j_{\rm pol}(z,t)$, can be calculated from the space-time–evolved quantum operator for the electron-positron field $\Psi(z,t)$. These densities are calculated from the expectation value of the corresponding operators as

$$\rho_{\rm pol}(z,t) \equiv \langle {\rm vac}|q[\Psi(z,t)^\dagger\Psi(z,t) - \Psi(z,t)\Psi(z,t)^\dagger]/2|{\rm vac}\rangle, \tag{2.4a}$$

$$j_{\rm pol}(z,t) \equiv \langle {\rm vac}|qc[\Psi(z,t)^\dagger\sigma_1\Psi(z,t) - \Psi(z,t)\sigma_1\Psi(z,t)^\dagger]/2|{\rm vac}\rangle. \tag{2.4b}$$

If we express the time evolution of the field operators in terms of $\Psi(z,t)$ and $\Psi(z,t)^\dagger$ by the solutions to the Dirac equation, we obtain [16]

$$\rho_{\rm pol}(z,t) = q\,\Sigma_p[W_p(d;z,t)^\dagger W_p(d;z,t) - W_p(u;z,t)^\dagger W_p(u;z,t)]/2, \tag{2.5a}$$

$$j_{\rm pol}(z,t) = qc\,\Sigma_p[W_p(d;z,t)^\dagger\sigma_1 W_p(d;z,t) - W_p(u;z,t)^\dagger\sigma_1 W_p(u;z,t)]/2, \tag{2.5b}$$

where each state is evolved under the Dirac Hamiltonian of Eq. (2.1). These solutions can be obtained on a space-time lattice with N_t temporal and N_z spatial grid points using a fast-Fourier-transformation–based split-operator scheme [17–21]. We truncated the energy sums Σ_p above a cut-off energy, denoted by $E_{\rm cut}$.

There are two different mathematical mechanisms by which each density vanishes initially. At the initial time $t = 0$, the states $W_p(u;z,t)$ and $W_p(d;z,t)$ are identical to the energy eigenstates defined in Eq. (2.2). As a result, each term $W_p(z,t)^\dagger W_p(z,t) = (2\pi)^{-1}$ is spatially constant and the difference of the (infinite) sums Σ_p over all states with positive and negative energies is zero, leading to $\rho_{\rm pol}(z,t=0) = 0$. As each energy is doubly degenerate, we have states with positive and negative current densities per energy. As a result, the vanishing total current density $j_{\rm pol}(z,t=0) = 0$ is based on a cancellation within each pair of degenerate energy states. The computation of $\rho_{\rm pol}(z,t)$ and especially $j_{\rm pol}(z,t)$ therefore requires us to truncate the momentum states symmetrically. We note that FFT-based grid methods naturally require an unbalanced manifold of momenta due to the Nyquist state.

It is also interesting that in this particular quantum-field theoretical framework the time evolution of states of initially positive free energy $W_p(u;z,t)$ seems to contribute to the positive sign of the charge density (note that $q = -1$ a.u.), whereas the negative energy states contribute with a negative sign. If we had replaced the initial bare vacuum state $|{\rm vac}\rangle$ in the expectation value in Eq. (2.4a) with a single electron state with momentum P, $|P\rangle$, the resulting time evolution of $\rho_{\rm pol}(z,t)$ would be identical to the solution given in Eq. (2.5a), except for an additional negative term $q\,W_P(u;z,t)^\dagger W_P(u;z,t)$, reflecting correctly the negative charge of an electron, which is simply superimposed on the vacuum's density. In the Dirac sea picture, the depletion (transition to positive energy states) of the negative energy states is usually associated with the occurrence of a positive charge (positron).

III. SIMPLE ANALYTICAL MODELS FOR $\rho_{\rm pol}(z,t)$ AND $j_{\rm pol}(z,t)$

In Sec. III A we outline a simple analytical model that permits us to predict the space-time evolution of the vacuum's polarization density for arbitrary configurations of static external fields. In Sec. III B we find another model that predicts this density for the case in which a charge was placed at location $z = 0$ at time $t = 0$. In contrast to the first case, where the steady-state electric field was established before the vacuum polarization began to develop, here the vacuum's polarization is established simultaneously with the propagating external field.

A. Formation of the vaccum's polarization in a given external field configuration

Here we assume that we have a given (time-independent) charge density $Q_{\rm ext}(z)$. According to the steady-state Maxwell equation $[-\partial_z{}^2 V_{\rm ext} = 4\pi\, Q_{\rm ext}(z)]$, this can be associated with an external (steady-state) scalar potential $V_{\rm ext}(z)$. The associated electric field $E_{\rm ext}(z)[= -\partial_z V_{\rm ext}(z)]$ induces a polarization charge density of the QED vacuum that we have denoted by $\rho_{\rm pol}(z,t)$. In the prior section we showed that this vacuum polarization density is obtained as a solution to the Dirac equation, which depends on the external potential $V_{\rm ext}(z)$. We argue below that one can find a new description in which the potential acts only as an intermediary agent and where the resulting time-evolved density $\rho_{\rm pol}(z,t)$ can be obtained *directly* from the original distribution of the externally given charge $Q_{\rm ext}(z)$. Similarly to an electromagnetic field, in this description the polarization charge density can be modeled by a simple wave equation, where a term that is proportional to $Q_{\rm ext}(z)$ acts as a source term:

$$\left(\partial_{ct}{}^2 - \partial_z{}^2\right)\rho_{\rm pol}(z,t) = 8\pi\,\chi_d\, Q_{\rm ext}(z). \tag{3.1}$$

This equation is just a postulate, whose validity needs to be established below. We denote the proportionality constant χ_d as the vacuum's linear susceptibility.

If we assume the two initial conditions $\rho_{\rm pol}(z,t=0) = \partial_t \rho_{\rm pol}(z,t=0) = 0$, the inhomogeneous solution reads

$$\begin{aligned}\rho_{\rm pol}(z,t) &= (c/2)\int_0^t dt' \int_{z-c(t-t')}^{z+c(t-t')} dz' [8\pi \chi_d Q_{\rm ext}(z')] \\ &= (c/2)\int_0^t dt' \int_{z-c(t-t')}^{z+c(t-t')} dz'\, 2\chi_d\big[-\partial_{z'}{}^2 V_{\rm ext}(z')\big] \\ &= -\chi_d c \int_0^t dt' \{\partial_z V_{\rm ext}[z+c(t-t')] - \partial_z V_{\rm ext}[z-c(t-t')]\} \\ &= -\chi_d \int_0^t dt' \{-\partial_{t'} V_{\rm ext}[z+c(t-t')] - \partial_{t'} V_{\rm ext}[z-c(t-t')]\} \\ &= \chi_d\,[2V_{\rm ext}(z) - V_{\rm ext}(z-ct) - V_{\rm ext}(z+ct)], \end{aligned} \tag{3.2}$$

where we have used $-\partial_{z'}{}^2 V_{\rm ext} = 4\pi Q_{\rm ext}$.

This simple solution can also be derived phenomenologically, if we assume that the corresponding external force on a charge q, $F_{\rm ext} = -q\partial_z V_{\rm ext}(z)$ plays two roles. First, it continuously separates the virtual electrons and positrons and then secondly, shifts them apart with velocities $\pm c$. If we postulate that the separated charge per unit time at each location is directly proportional to the external force, then the accumulated charge would simply grow linearly in time, $\chi_d\, E_{\rm ext}(z)t$. However, in a region where $E_{\rm ext}(z) > 0$, the virtual positrons [associated with the positive portion of $\rho_{\rm pol}(z)$] evolve with a speed c to the left whereas virtual electrons move to the right, leading to the instantaneous density proportional to $\{E_{\rm ext}[z+ct] - E_{\rm ext}[z-ct]\}$. If we sum (integrate) over layers separated at different creation times t', we would obtain $\rho_{\rm pol}(z,t) = \chi_d\, c \int^t dt' \{E_{\rm ext}[z + c(t-t')] - E_{\rm ext}[z-c(t-t')]\}$. Furthermore, if we use $E_{\rm ext}(z) = -\partial_z V_{\rm ext}(z)$ and $\partial_{ct} A_{\rm ext}(z) = 0$, this expression can be simplified to the solution given by Eq. (3.2).

In one spatial dimension the corresponding electric current density can be determined directly from the charge-density solution (3.2) using the continuity equation $\partial_z j_{\rm pol}(z,t) = -\partial_t \rho_{\rm pol}(z,t)$. If we replace $\partial_t V_{\rm ext}(z \pm ct)$ by $\pm\partial_z V_{\rm ext}(z \pm ct)c$ and assume $j(z,t=0) = 0$, we obtain

$$j_{\rm pol}(z,t) = \chi_d c[V_{\rm ext}(z+ct) - V_{\rm ext}(z-ct)]. \tag{3.3}$$

In order to test the numerical accuracy of this remarkably simple model, we have used two external scalar potentials. The first one, $V_{\rm ext}(z) = -Q2\pi|z|$, describes a steady-state electric field $E(z) = -Q2\pi + Q4\pi\, U(z)$ associated with a spatially localized point charge $Q_{\rm ext}(z) = Q\delta(z)$. Here and below we denote with U a generalized unit step function that is 1 if each argument is positive and vanishes if any argument is negative. We neglect here the fact that in quantum-field theory a charge density cannot be localized within more than the electron's Compton wavelength [22,23], which is much smaller than the spatial range of interest here. We will return to this important point in Sec. III C.

If we insert the specific form $V_{\rm ext}(z) = -Q2\pi|z|$ into Eq. (3.2), we obtain $\rho_{\rm pol}(z,t) = \chi_d Q4\pi\,(ct - |z|)\,U(ct - |z|)$ and similarly, from Eq. (3.3) we obtain $j_{\rm pol}(z,t) = \chi_d Q4\pi\,[zU(ct-|z|) + t|z|/z\; U(|z| - ct)]$. The spatially constant but temporally growing portion of $j_{\rm pol}(z,t)$ outside the light cone ($|z| > ct$) confirms that the constant electric field $E_{\rm ext} = 2\pi Q|z|/z$ can separate the charges everywhere in space with equal strength. In order to obtain the total induced charge around $z = 0$, we integrate $\rho_{\rm pol}(z,t)$ and obtain $Q_{ind}(t) = \int dz \rho_{\rm pol}(z,t) = \chi_d Q4\pi\, t^2$.

In Fig. 1 we compare the dynamics of the charge and current densities from Eqs. (3.2) and (3.3), with the exact ones obtained numerically from the full quantum-field theoretical calculation via Eq. (2.4). We found that for charges $Q < 10^5$ a.u., the agreement is superb.

There are five observations in order. First, we note that the current density $j_{\rm pol}(z,t)$ is a better diagnostic tool to examine the polarization dynamics than $\rho_{\rm pol}(z,t)$. While the charge

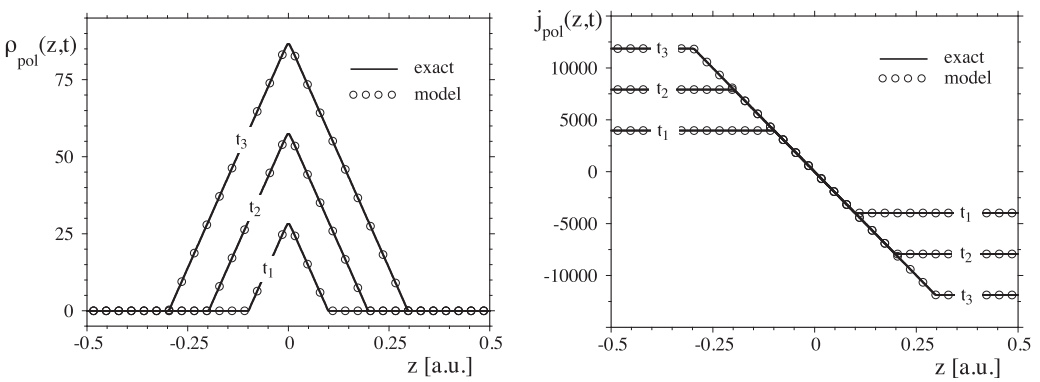

FIG. 1. Three snapshots of the vacuum's charge (left) and current (right) spatial densities $\rho_{\rm pol}(z,t)$ and $j_{\rm pol}(z,t)$ induced by the (long-range) electric field of a positive charge $Q = 2\times 10^4$ placed at $z = 0$. The three times are $t_n = n \times 0.1/c$. For comparison, the circles are the model densities obtained from Eqs. (3.2) and (3.3). [The numerical parameters are the box length $L = 1.6$ a.u., the number of temporal grid points $N_t = 400$, the number of spatial grid points $N_z = 1024$, and the cut-off energy was chosen $E_{\rm cut} = 7.3c^2$.]

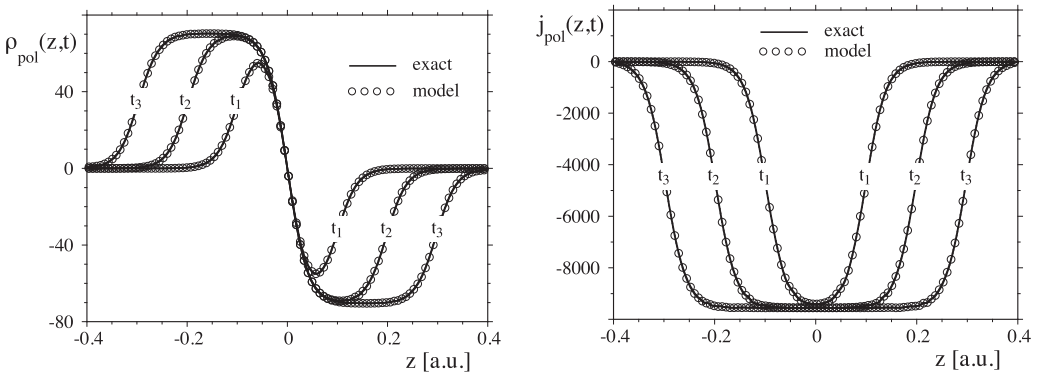

FIG. 2. Three snapshots of the vacuum's charge (left) and current (right) spatial densities $\rho_{\rm pol}(z,t)$ and $j_{\rm pol}(z,t)$ induced by the (short-range) electric field of a dipole distribution. The three times are $t_n = n \times 0.1/c$. The positive (negative) charge cloud Q was placed at $z = -0.658w$ $(0.658w)$. The corresponding external potential is given by a smooth barrier $V_{\rm ext}(z) = V_0[1 + \tanh(z/w)]/2$, with $V_0 = 6 \times 10^4$ and $w = 0.04$ a.u. For comparison, the circles are the model densities obtained from Eqs. (3.2) and (3.3). [Parameters are $L = 1.6$ a.u., $N_t = 400$, $N_z = 1024$, $E_{\rm cut} = 7.3c^2$.]

density seems to originate from the location of the field-generating charge $Q_{\rm ext}$, the current density grows simultaneously everywhere, while the total charge density remains zero outside the light cone (defined by $z = \pm ct$). The nonvanishing $j_{\rm pol}(z,t)$ nicely illustrates the interpretation of a separation of opposite charges and their subsequent motion in opposite directions, as assumed in the justification of our model.

Second, while real physical electrons and positrons have a finite mass 1 a.u., the polarization density propagates precisely with the speed of light, as already suggested by the arguments $z \pm ct$ in Eqs. (3.2) and (3.3). This is even true if the external field was due to an arbitrarily small external charge $Q_{\rm ext}$, whose associated electric force field would take forever to accelerate a single physical electron or positron to a speed close to c.

The third observation concerns the sign of the polarization charge density. While we chose a positive external charge $Q_{\rm ext}$, the polarization charge is positive close to it, as if the virtual positrons are attracted by it. This counterintuitive behavior was already noticed in the early 1970s by Greiner and colleagues. The same behavior is observed if instead of Eq. (2.4a) the density was computed from the unsymmetrized form $\langle {\rm vac}|\, q\Psi(z,t)^\dagger\, \Psi(z,t)\,|{\rm vac}\rangle$, except that here we have to subtract out the infinite back ground value $\langle {\rm vac}|\, q\Psi(z=\infty,t)^\dagger\, \Psi(z=\infty,t)\,|{\rm vac}\rangle$. We will return to this rather puzzling point in Sec. IV, where, in addition to the polarization based on the separation of virtual particles, real physical particles are produced which show the expected opposite behavior.

Fourth, the accumulation of positive charges close to $z = 0$ is accompanied by an equal but opposite density close to the physical boundaries of our numerical box (not shown in the figure). So the total charge is actually conserved, as expected.

Fifth, the fact that the polarization growth continues forever is expected, as in this simulation we have assumed the presence of an external (permanent) charge $Q_{\rm ext}$. The unexpected effect of any backreaction (as described by the Maxwell equation) is addressed in Sec. V.

Let us now study a second test case for the model predictions of $\rho_{\rm pol}(z,t)$ and $j_{\rm pol}(z,t)$,where we chose a dipole distribution of 2 localized by finitely extended charge clouds with total charge $\pm Q$, each that are about 1.3 w apart from each other. The corresponding potential is short range and given by a smooth potential barrier $V_{\rm ext}(z) = V_0[1 + \tanh(z/w)]/2$ with an amplitude $V_0 = 8\pi Q/w$ and spatial width w [24,25]. The charge density associated with this potential $[Q_{\rm ext}(z) = -\partial_z{}^2\, V_{\rm ext}/(4\pi)] = V_0\,{\rm sech}(z/w)^2\tanh(z/w)/(4\pi w^2)$ has its extremes at $z = \pm{\rm arcsech}[(2/3)^{1/2}]w = \pm 0.658w$, with a total area $\int dz\,|Q_{\rm ext}(z)| = 2Q$.

In Fig. 2 we compare the (numerically) determined polarization charge and current densities for the short-range field with the model predictions according to Eqs. (3.2) and (3.3). The agreement is again excellent. In contrast to the infinite growth of $\rho_{\rm pol}(z,t)$ and $j_{\rm pol}(z,t)$ for the long-range case, the short-range field induces only a finite polarization that propagates with speed c to $z = \pm\infty$.

In Figs. 1 and 2 we have used the ratio of the predicted and exact densities to determine the unknown proportionality factor χ_d, which we can associate with the dynamical linear susceptibility for the one-dimensional QED vacuum. We find the same numerical value $\chi_d = 1.15 \times 10^{-3}$ a.u. for both systems. We should stress that this value for a dynamical situation is different from the one obtained from static considerations, as we discuss below in Sec. III C. For the dipole field we have varied the amplitude from $V_0 = 1000$ to 6×10^4 for $w = 0.04$ a.u. and found that precisely the same value $\chi_d = 1.15 \times 10^{-3}$ a.u. describes the entire range rather accurately.

B. The formation of a polarization in a given external charge configuration

In our first model we have assumed that the field-generating charge $Q_{\rm ext}(z)$ was created at time $t = -\infty$, such that the resulting electric field had sufficient time to reach its asymptotic distribution $V_{\rm ext}(z)$ before we allowed the vacuum to begin to react to it at time $t = 0$. We note that this situation is generic to most QED calculations that use the external strong field approximation.

In this section we analyze the case where the external charge Q is placed at $z = 0$ at time $t = 0$. By solving the Maxwell equation $(\partial_{ct}{}^2 - \partial_z{}^2)V_{\rm ext}(z,t) = 4\pi\, Q\delta(z)$ with $V_{\rm ext}(z, t = 0) = \partial_t V_{\rm ext}(z, t = 0) = 0$, we obtain the solution

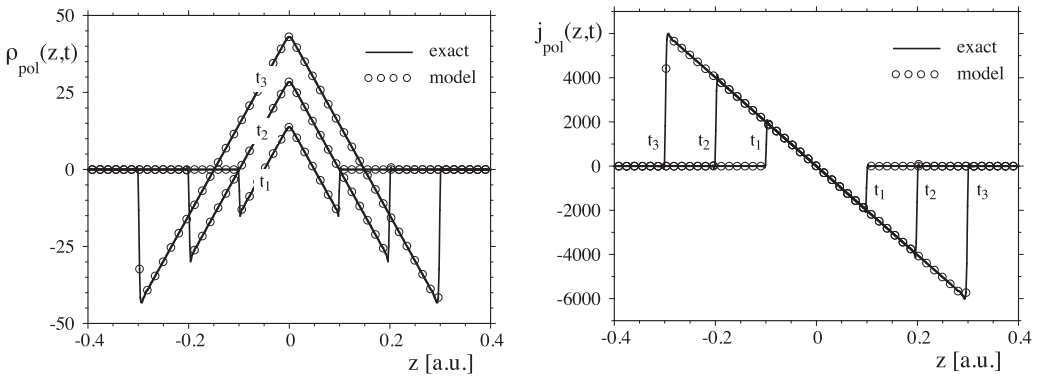

FIG. 3. Three snapshots of the vacuum's charge (left) and current (right) spatial densities $\rho_{\rm pol}(z,t)$ and $j_{\rm pol}(z,t)$ induced by a positive charge $Q = 2 \times 10^4$ placed at $t = 0$ at location $z = 0$. In contrast to the data in Fig. 1, here the external field is not established at $t = 0$. The three times are $t_n = n \times 0.1/c$. For comparison, the circles are the model densities obtained from Eqs. (3.5). [Parameters are $L = 1.6$ a.u., $N_t = 400$, $N_z = 1024$, $E_{\rm cut} = 7.3c^2$.]

describing the propagation of the external field,

$$V_{\rm ext}(z,t) = Q(-2\pi|z| + 2\pi ct)U(ct - |z|). \tag{3.4}$$

In the asymptotic long-time limit $t \to \infty$, the unit step function $U(ct - |z|)$ becomes 1 for all finite z, and if we subtract the infinite (physically irrelevant and spatially constant) $V(z = 0,t) = 2\pi\, cQt$ from this potential, we obtain the simpler asymptotic form $V_{\rm ext}(z,t \to \infty) = -2\pi Q|z|$, which we have used above. Generalizing our modeling technique to a time-dependent external potential, we postulate the solutions for the induced charge and current density to be

$$\rho_{\rm pol}(z,t) = \chi_d Q(-4\pi|z| + 2\pi ct)U(ct - |z|), \tag{3.5a}$$

$$j_{\rm pol}(z,t) = \chi_d Qc(-2\pi z)U(ct - |z|). \tag{3.5b}$$

As we believe that the polarization density is linear in the charge, the more complicated polarization density induced by an entire distribution of charges can be obtained by summing the individual contributions.

We note that the limit $t \to \infty$ in Eq. (3.5a) suggests that we have again an infinite buildup of a positive charge density at the location of the external charge, $\rho_{\rm pol}(z = 0,t) = \chi_d Q2\pi ct$. In Fig. 3 we have established the validity of the postulate Eq. (3.5) based on the *same* dynamical susceptibility $\chi_d = 1.15 \times 10^{-3}$ a.u. We see that in contrast to the data in Fig. 1 for an infinitely extended external potential, in Fig. 3 ρ as well as j vanish outside the light cone, which is fully consistent with causality. Therefore the polarization density instantaneously follows the propagating external force field due to the central charge.

C. The vacuum's polarization density for the steady-state limit

The polarization of the vacuum is usually discussed within a nondynamical static context in which the density does not evolve in time. As there are already some works about this subject [3,26], for completeness we only briefly review here the steady-state polarization for those two specific field configurations discussed in this work. To obtain the densities for the fully dressed (interacting) vacuum state $|{\rm VAC}\rangle$, it is advantageous to expand the field operator in Eqs. (2.3) in terms of the creation and annihilation operators for physical (not bare) electrons and positrons. When these operators act on the dressed vacuum state $|{\rm VAC}\rangle$, the energy eigenstates of the coupled Dirac Hamiltonian [which contains $V_{\rm ext}(z)$] are getting occupied. In terms of these energy eigenstates, the steady-state densities are then obtained as

$$\rho_{\rm pol}(z) = q\Sigma_p[F_p(d;z)^\dagger F_p(d;z) - F_p(u;z)^\dagger F_p(u;z)]/2, \tag{3.6a}$$

$$j_{\rm pol}(z) = qc\Sigma_p[F_p(d;z)^\dagger\sigma_1 F_p(d;z) - F_p(u;z)^\dagger\sigma_1 F_p(u;z)]/2. \tag{3.6b}$$

These expressions are formally similar to Eqs. (2.5), but here the states $F_p(z)$ are the energy eigenstates of the coupled Hamiltonian that includes the external potential $V_{\rm ext}(z)$. As a result, these densities do not change when each state is (trivially) evolved under the Dirac Hamiltonian. Also note that in contrast to the states $W_p(z,t)$ of Eqs. (2.4), a distinction between up-states $F_p(u;z)$ (with energy greater than $-c^2$) and down-states $F_p(d;z)$ (with energy less than $-c^2$) is no longer possible when the potential is so strong that the two energy manifolds begin to overlap with each other. This agrees, of course, with the onset condition of supercritical behavior characteristic of the creation of new particles [9].

The required eigenstates can be obtained numerically by diagonalizing the Hamiltonian in an appropriate representation. We found that even though we used just a two-point finite difference formula for the momentum operator on a spatial grid (which also leads to the well-known fermion doubling problem), the eigenvectors were numerically useful, not even requiring any energy cutoff for our parameters. In fact, the entire Hilbert space had to be taken into account to obtain convergent results. In Ref. [26] we have derived an approximate analytical scheme that suggests that the density $\rho_{\rm pol}(z,t)$ is directly proportional to the second derivative of the external potential,

$$\rho_{\rm pol}(z) = \alpha_s \partial_z{}^2 V_{\rm ext}(z). \tag{3.7}$$

Based on the nonrelativistic limit, the numerical value of this static susceptibility was derived in Ref. [26] to take the value $\alpha_s = [4(1 + \sqrt{2})c^3]^{-1} = 4 \times 10^{-8}$ a.u.

In Fig. 4(a) we have computed the exact steady-state polarization density based on Eq. (3.6) for our external field

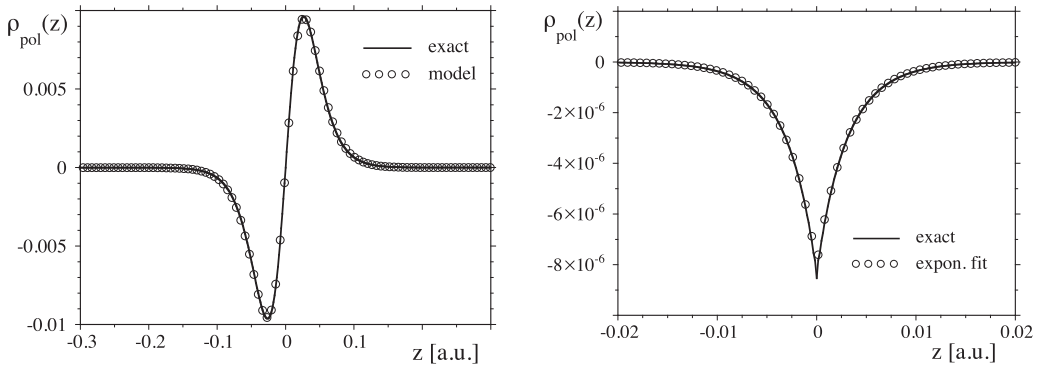

FIG. 4. The steady-state polarization density $\rho_{\rm pol}(z)$ associated with the external charge distribution of a dipole (a) and a sharply located charge at $z = 0$ (b) obtained from the eigenvectors of the Dirac Hamiltonian with an external potential $V_{\rm ext}(z)$. The corresponding external potentials are $V_{\rm ext}(z) = V_0[1 + \tanh(z/w)]/2$, with $V_0 = 1000$ and $w = 0.04$ a.u., and $V_{\rm ext}(z) = -Q2\pi|z|$ with $Q = 0.1$ a.u. For comparison, the circles in the left figure are the model densities predicted according to Eqs. (3.7) and (3.8). [Numerical parameters are $L = 1.6$ a.u., $N_z = 1000$, no energy cutoff.]

describing the dipole charge distribution. The agreement with the analytical formula Eq. (3.7) is again excellent. In direct contrast to the finding about the dynamical polarization, we observe (and fully consistent with a prior work [26]) that the positive virtual charge cloud is attracted to those spatial regions where the external charge is negative, similar to the true attraction among real physical particles of opposite charges. As we have indicated above, the density of the external charge configuration density associated with this potential is given by the steady-state Maxwell equation, $Q_{\rm ext}(z) = -\partial_z{}^2 V_{\rm ext}/(4\pi)$. Combining this with our analytical estimate of Eq. (3.7), we obtain

$$\rho_{\rm pol}(z) = -\alpha_s 4\pi\, Q_{\rm ext}(z). \tag{3.8}$$

In other words, up to the overall universal reduction factor of $4\pi\alpha_s = 5 \times 10^{-7}$ a.u., the spatial distribution of the induced polarization charge density of the dressed vacuum is identical to the original external charge distribution, except the reversed sign. For comparison, the amplitude of the dynamical polarization density [see Fig. 2 and Eq. (3.3)] was $\rho_{\rm pol}(z,t \to \infty) = \chi_d V_0$. We have shown above the relationship of amplitude to the charge and the width w of the charge distribution, $V_0 = 8\pi Q/w$. In other words, we have $\rho_{\rm pol}(z,t \to \infty) = (\chi_d 8\pi/w)Q$, representing an attenuation factor $(\chi_d 8\pi/w)$ that, in contrast to $4\pi\alpha_s$, does depend on the distribution of the external charge configuration.

In Fig. 4(b) we have shown the steady-state polarization charge density induced by a single sharply localized charge Q at $z = 0$, corresponding to $Q_{\rm ext}(z) = Q\delta(z)$ and $V_{\rm ext}(z) = -2\pi Q|z|$. This is an interesting case, as the second spatial derivative of the potential vanishes here except at $z = 0$, and quantum-field theory cannot predict a sharply localized charge density, $\rho(z) \neq Q\delta(z)$. In prior works it was suggested [22,23] that the narrowest probability and also charge distribution that can be predicted by relativistic quantum-field theory has to have a minimum extension given by the electron's Compton wavelength, $1/c$. This expectation is nicely confirmed by the graph in Fig. 4(b), where the spatial profile of the induced charge density is very well matched by the numerically fitted density $\rho_{\rm ext}(z) = 8 \times 10^{-6} \exp(-2.3c|z|)$.

We note that the corresponding current density for the dressed vacuum is always zero. This is fully consistent with the continuity equation and the fact that the polarized virtual charges in the dressed vacuum are not moving in the steady state.

IV. THE EFFECT OF THE CREATION OF REAL PHYSICAL PARTICLES ON THE POLARIZATION

We have seen above that the analytical expressions for $\rho_{\rm pol}(z,t)$ and $j_{\rm pol}(z,t)$ describe the space-time evolution rather accurately, if the external fields are not too strong and if we use the numerical value of $\chi_d = 1.15 \times 10^{-3}$ a.u. for the dynamic linear susceptibility of the vacuum. In this section we will decrease the distance w between the two external charges for the dipole configuration discussed above such that the associated electric field is increased. There are two different mechanisms that will lead to possible discrepancies between the exact densities and those postulated by the simple linear model of Eqs. (3.2) and (3.3). The first one is due to the true nonlinear nature of the relationship between the external field and the induced charge for sufficiently large electric fields. In this case most likely higher-order susceptibilities need to be invoked, but it is not clear how the simple wave-equation-based model can be generalized.

The second cause for the inapplicability of the model is the irreversible breakdown of the vacuum, as indicated by the occurrence of real electron-positron pairs that are continuously generated. This will happen if two criteria are fulfilled. First, the potential has to be supercritical, i.e., V_0 has to exceed twice the rest mass of the electron, $V_0 > 2c^2$. Second, in order for an appreciable particle flux to be present, we also require that the associated electric field is sufficiently large, which for a given V_0 can be accomplished by chosen a small distance w, which we have done.

In Fig. 5 we show how the generation of these physical particles affects the final polarization charge and current densities of the vacuum. We see that the charge density is *decreased* significantly compared to the model prediction if the strength of the potential exceeds $V_0 = 2c^2$. The data in

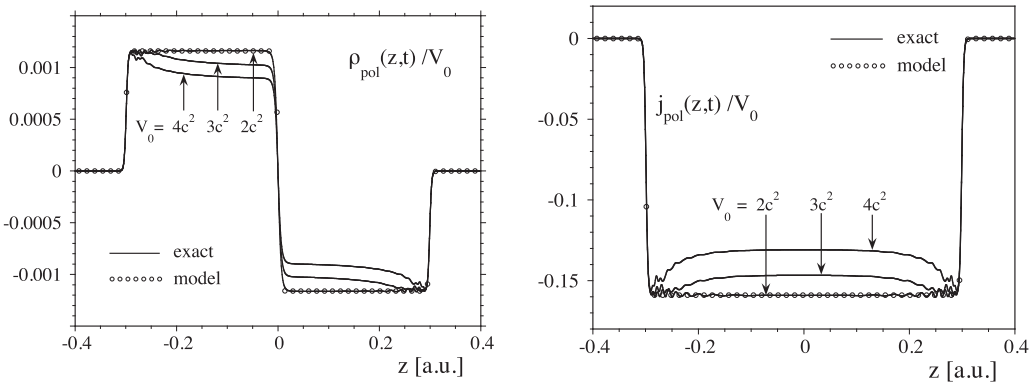

FIG. 5. Comparison of the exact the vacuum's charge (left) and current (right) densities $\rho_{\rm pol}(z,t)$ and $j_{\rm pol}(z,t)$ induced by the (short-range) electric field of a dipole distribution and the predictions of Eqs. (3.2) and (3.3) in the pair-creation regime. The interaction time was $t = 0.3/c$. The corresponding external potential is given by $V_{\rm ext}(z) = V_0[1 + \tanh(z/w)]/2$ with $w = 0.5/c$ a.u. For better comparison the graphs were divided by V_0. The circles are the model densities obtained from Eqs. (3.2) and (3.3). [Parameters are $L = 1.6$ a.u., $N_t = 800$, $N_z = 2048$, $E_{\rm cut} = 14.6c^2$.]

Fig. 5 were computed for $V_0 = 2c^2$, $3c^2$, and $4c^2$, leading to a total number of created particles of 0.063, 1.63, and 4.76, respectively, after the interaction. We show below that the decrease of the observed charge as well as current density is directly related to the occurrence of real physical electrons and positrons. In direct contrast to the virtual electrons (positrons) that are ejected to the right (left) of the dipole field, the created physical particles evolve in the *opposite* direction. This behavior of the real particles is fully expected, as the positive charge that causes the dipole field is centered around $z = -w$ while the negative charge is at $z = w$. The created electrons (positrons) are accelerated between the charges at $z = \pm w$ to the left (right).

In Fig. 6 we display the time evolution of the charge and current densities for the same parameters as in Fig. 5 and $V_0 = 3c^2$. To reduce the spatial oscillations following the front edge of the densities shown in Fig. 5, we have turned the external potential on smoothly for a time interval $T_{\rm on} = 0.02/c$. As a result, the front edge is also less steep but still almost entirely associated with the propagating vacuum's polarization charge. Only after a time does the dipole region turn into a source for a constant flux, as also indicated by the current density displayed in the right Fig. 6.

To examine the relationship between the vacuum polarization and the pair creation more quantitatively, we have computed the mass density of the created real electrons and positrons directly [16,22]. The total charge density $\rho_{\rm pol}(z)$ does not allow us to distinguish between the density of the individual electrons and positrons. For example, if an electron and a positron have identical spatial probability densities, then the total charge density is zero, as if there were no particles at all. It is therefore not possible to compute the total number of created electron-positron pairs directly from $\rho_{\rm pol}(z)$. In order to be able to distinguish both cases, we have to compute also a spatial probability density for both particles. Consistent with prior works [16], we define spatial probability densities that are based on the assumption that we can separate the total electron-positron field operator into a positronic and electronic portion $\Psi(z,t) = \Psi(e^-;z,t) + C\Psi(e^+;z,t)$ using the charge-conjugation operator C. This definition of $\Psi(e^-;t)$ allows us to compute the total number of particles as well as the spatial particle number density of the created electrons and

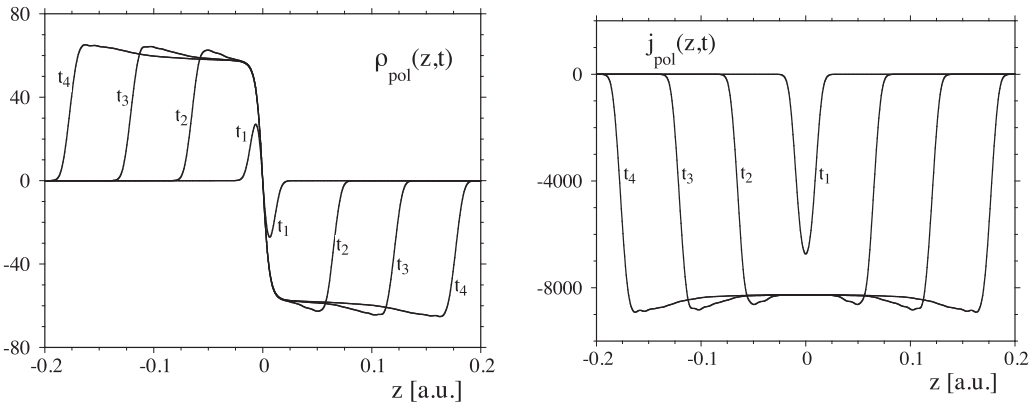

FIG. 6. Four snapshots of the vacuum's charge (left) and current (right) spatial densities $\rho_{\rm pol}(z,t)$ and $j_{\rm pol}(z,t)$ induced by the (short-range) electric field of a dipole distribution corresponding to an external potential $V_{\rm ext}(z) = V_0[1 + \tanh(z/w)]/2$ with $w = 0.5/c$ a.u. and $V_0 = 3c^2$. The four times are $t_n = (3n - 2)\ 1.37 \times 10^{-4}$ a.u.. [Parameters are $L = 1.6$ a.u., $N_t = 800$, $N_z = 2048$, $E_{\rm cut} = 14.6c^2$, $T_{\rm on} = 0.02/c$.]

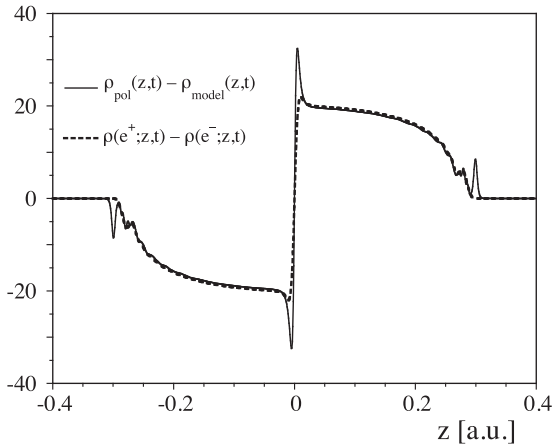

FIG. 7. Comparison of the charge density that is exclusively associated with created real electrons and positrons, defined as $\rho(e^+;z,t) - \rho(e^-;z,t)$, and the difference between the total observed charge density $\rho_{\rm pol}(z,t)$ and its analytical model estimate of Eq. (3.2). The dynamics is the same as in Fig. 5 for $V_0 = 4c^2$. [Parameters are $L = 1.6$ a.u., $N_t = 1600$, $N_z = 2048$, $E_{\rm cut} = 14.6c^2$.]

positrons:

$$\rho(e^-;z,t) = \langle \mathrm{vac}|\Psi(e^-;z,t)^\dagger \Psi(e^-;z,t)|\mathrm{vac}\rangle, \quad (4.1a)$$

$$\rho(e^+;z,t) = \langle \mathrm{vac}|\Psi(e^+;z,t)^\dagger \Psi(e^+;z,t)|\mathrm{vac}\rangle. \quad (4.1b)$$

If we use again the time-evolved Hilbert space states and the matrix elements of the time evolution operator $U(t)$ between them, we can calculate these densities as

$$\rho(e^-;z,t) = \Sigma_{p'}|\Sigma_p \langle u;p|U(t)|d;p'\rangle W_p(u;z)|^2, \quad (4.2a)$$

$$\rho(e^+;z,t) = \Sigma_{p'}|\Sigma_p \langle d;p|U(t)|u;p'\rangle W_p(d;z)|^2. \quad (4.2b)$$

In Fig. 7 we have taken the data from Fig. 5 for $V_0 = 4c^2$ and graphed for each location z the difference between the exact density $\rho_{\rm pol}(z,t)$ and the prediction of our simple model $\rho_{\rm model}(z,t) = \chi_d[2V_{\rm ext}(z) - V_{\rm ext}(z - ct) - V_{\rm ext}(z + ct)]$. These data are shown together with the corresponding charge density, that is exclusively associated with the created real particles and defined as

$$\rho_{\rm real}(z,t) \equiv \rho(e^+;z,t) - \rho(e^-;z,t). \quad (4.3)$$

The agreement between both curves is superb and clearly confirms that the main modification of the polarization density can be directly associated with the creation of real electron-positron particle pairs. We note that in contrast to the virtual particles that propagate with the speed of light c, leading to the spatially constant density, the created physical particles are massive and evolve with a distribution of velocities bound by c. As a result, the front portion of the density $\rho_{\rm real}(z,t)$ contains fewer particles and is more curved than the practically rectangular-shaped $\rho_{\rm pol}(z,t)$. We also note that the spatial integral over $\rho(e^-;z,t)[\rho(e^+;z,t)]$ is identical to the number of created electrons [positrons] after the interaction. The spike in the front portions of $\rho(e^-;z,t)[\rho(e^+;z,t)]$ is a well-known phenomenon and is associated with the temporally induced pair creation [27,28] due to the sudden turn-on of the external potential. The difference inside the dipole region $-w < z < w$ is more difficult to interpret [29], as the very definition of $\rho(e^+;z,t) - \rho(e^-;z,t)$ is based on the projection on field-free energy eigenstates and therefore can be interpreted unambiguously as a real particle density only outside the supercritical region, $z < -w$ and $w < z$.

V. THE EFFECT ON POLARIZATION DUE TO THE INTERACTION AMONG VIRTUAL PARTICLES

So far each calculation above has excluded the backreaction of the induced charge clouds on the internal electric fields. As a result, the virtual as well as created electron-positron pairs were not able to interact with each other, despite their charges. A fundamentally correct description would require us to take the photon as a second-quantized particle into account. Unfortunately, this is presently beyond computational feasibility. However, if the interacting field is approximated by a classical field whose evolution is governed by the Maxwell equations, the interfermionic forces can be modeled [30–32]. The accuracy of this approximation, however, is presently not known. In a recent work we have pointed out [32] that the unavoidable self-energy in this approach can lead to an unphysical self-repulsion of a single electron, whose significance is still not clear. While a single electron or positron modeled by a quantum-mechanical wave function should not be able to interact with itself, the present description permits such an "unphysical" interaction due to the intrinsic statistical meaning of a wave packet. While according to the Born interpretation the spatial probability density represents only a temporal average of infinitely many measurements of the same single particle, in our approach (where the Maxwell field was not second quantized) the whole spatial density acts as a source term in Maxwell equations, which then produces a field with which all portions of the wave function act simultaneously. In other words, different portions of the same particle wave packet can interact with themselves like particles in a classical ensemble of many particles or in a charge cloud.

We would like to point out that our model described in Sec. III A leads to an interesting coupled set of inhomogeneous wave equations. The wave equation (3.1) replaced the quantum-field theoretical Dirac equation for the charge density $\rho_{\rm pol}(z)$. If we replace the source term $Q_{\rm ext}(z)$ in Eq. (3.1) by $-\partial_z{}^2 V/(4\pi)$ we obtain

$$\left(\partial_{ct}{}^2 - \partial_z{}^2\right)\rho_{\rm pol}(z,t) = -2\chi_d \partial_z{}^2 V(z), \quad (5.1a)$$

$$\left(\partial_{ct}{}^2 - \partial_z{}^2\right)V(z,t) = 4\pi\rho_{\rm pol}(z,t), \quad (5.1b)$$

where the Maxwell equation (5.1b) (in the Lorenz gauge) determines the potential $V(z,t)$ for a given charge distribution $\rho_{\rm pol}(z,t)$. While the validity of the source term $V(z)$ of Eq. (5.1a) has only been established above for a time-independent potential, the set of equations can be used to show that it could be possible to find only a spatially oscillatory steady-state polarization density that fulfills simultaneously the Dirac as well as Maxwell equations. For a true steady (nonpropagating) state polarization, we would require $\partial_{ct}{}^2\rho_{\rm pol}(z,t) = \partial_{ct}{}^2 V(z,t) = 0$, leading to $\partial_z{}^2\rho_{\rm pol}(z) = -8\pi\chi_d\rho_{\rm pol}(z)$. This equation, however, has only an infinitely extended oscillatory solution.

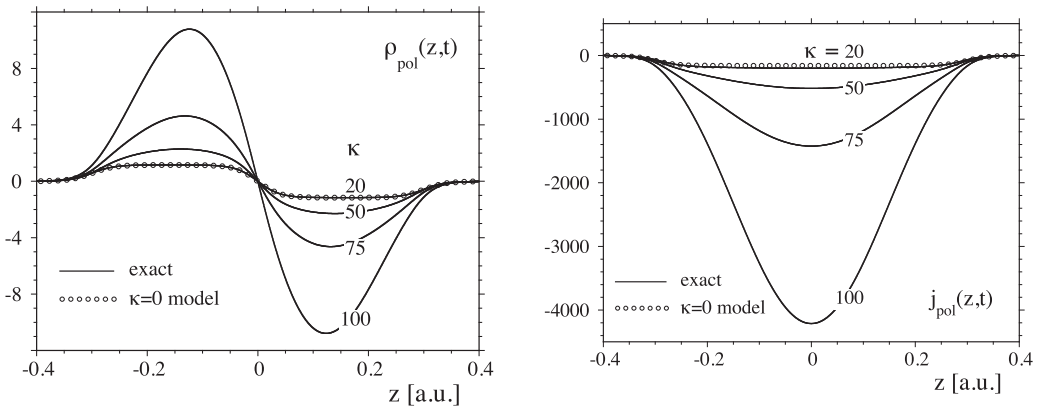

FIG. 8. Impact of the electron-positron, electron-electron, and positron-positron forces on the vacuum's charge (left) and current (right) densities $\rho_{\rm pol}(z,t)$ and $j_{\rm pol}(z,t)$ induced by the (short-range) electric field of a dipole distribution. The parameter κ is the interfermionic coupling strengths. The circles are predictions of Eqs. (3.2) and (3.3) that exclude any particle-particle interaction. The interaction time was $t = 0.3/c$. The corresponding external potential is given by $V_{\rm ext}(z) = V_0[1 + \tanh(z/w)]/2$ with $w = 0.04$ a.u. and $V_0 = 10^3$ a.u.. [Parameters are $L = 1.6$ a.u., $N_t = 8000$, $N_z = 2048$, $E_{\rm cut} = 7.37c^2$.]

In order to examine the effect of the coupling to the Maxwell equation on the dynamical polarization density, we have repeated the simulation leading to the data shown in Fig. 2, but we have introduced the coupling to the Maxwell equations as described by Eqs. (2.3). In order to emphasize the effect of the interaction among the virtual particles, we have introduced a dimensionless scaling parameter κ between the charge and current densities obtained from the Dirac equation and source terms required for the right-hand side of the Maxwell equations (2.3): $Q(z,t) = \kappa\rho_{\rm pol}(z,t)$ and similarly, $J(z,t) = \kappa j_{\rm pol}(z,t)$. As this effectively determines the charge of the virtual pairs, we have for reasons of consistency included κ also as prefactors for $V(z,t)$ and $A(z,t)$ in the Dirac equation.

In Fig. 8 we illustrate the impact of the virtual electron-electron, positron-positron, and electron-positron forces on the polarization process. We see that if the coupling strength exceeds $\kappa = 20$, $\rho_{\rm pol}(z,t)$ as well as $j_{\rm pol}(z,t)$ are significantly enhanced. As we presently do not have any physical intuition for these virtual particles, it is hard to say if this result is expected or not. We reiterate that these "particles" (or better, solutions to the Dirac equation) seem to evolve like massless particles with the speed of light and accumulate around an external charge of equal sign.

VI. SUMMARY AND OUTLOOK

In this work we have shown that the dynamical response of the bare fermionic Dirac vacuum in one spatial dimension to an external charge can be characterized by numerical susceptibilities χ_d. It turns out that quantum-field theoretical formation of the electric charge and current polarization densities of the bare vacuum due to an external charge distribution can be modeled by a remarkably simple inhomogeneous wave equation in which the external charge configuration acts as a source term. We have also shown how the predictions of this model need to be modified, when either real physical electron-positron pairs are created (for strong external fields) or if the mutual interaction of the virtual electrons and positrons is taken into account by the Maxwell equations. Many new questions need to be addressed in future works.

While the agreement between the model predictions and the accurate numerical solutions to the full quantum-field theoretical treatment is of astonishing accuracy, we would like to point out that we actually have not *derived* these equations from first quantum electrodynamical principles. As a result, the numerical value of the vacuum's dynamical linear susceptibility χ_d was simply obtained from a numerical fit of the exact data. The numerical value of the static susceptibility α_s, obtained from the physical (not bare) vacuum state, can be derived analytically [26]. Especially in view of an important possible generalization of this model to spatially three-dimensional systems, it would be very worthwhile to examine if a rigorous theoretical derivation from first principles could be developed.

We presently also do not understand if the initial bare vacuum state would evolve under the influence of an external charge to the physical (steady-state) vacuum state. This question is interesting, as in the dynamical context (consistent with Ref. [33]) the positively charged virtual particles seem to gather around a positive external charge, while in the steady state of the dressed vacuum, we observe the opposite tendency.

We should note that the observed buildup of the induced positive charges around the positive external charge and the resulting increase of the total electric field does not violate energy conservation. As an example, in the temporal gauge, the field energy $\frac{1}{8\pi}\int dz E^2(z,t)$ grows in time while the sum of the particle's free and interaction energy shrinks.

While the peculiar Coulomb force law in only one spatial dimension could be responsible for some of the features (distance-independent forces, finite polarization density at $z = \pm\infty$, etc.), the solutions to the wave equations could be generalized to two and three dimensions. But here their validity needs to be established with exact numerical solutions to the coupled Dirac-Maxwell equations that are computationally difficult in three dimensions at the moment.

Due to the unavoidable self-repulsion of a single electron wave packet due to the coupling to the Maxwell equation [32], it is still not clear and extremely difficult to analyze how accurate it actually is to replace the second-quantized photon

field operator by a simple classical Maxwell field to model the interaction among virtual and especially physical electrons and positrons. This problem might also manifest itself in the fact that the coupled Dirac-Maxwell equations in our model for the polarization density cannot predict any localized steady-state solutions.

We should mention that formation of the vacuum's polarization density can be studied even for a second-quantized photon field if we assume that the masses of the fermions vanish. In this one-dimensional Schwinger model of QED, the screening of charges due to the vacuum polarization can be examined analytically [34]. For this model it is even possible to compute an analytical expression for the electric conductivity of the one-dimensional vacuum [35] that relates the electric field to the induced polarization current.

While it is clear that the unavoidable occurrence of the propagating vacuum polarization charge and current density can play a major role in *ab initio* computations for massive fermions and therefore requires a better understanding, the main question concerns whether these currents can have a direct experimental signature. We are hopeful and point to the rather promising recent developments of very-high-intensity laser sources at numerous institutions [36–46] that aim at probing the basic structure of the quantum vacuum and might verify various predicted new phenomena, such as photon-photon scattering [47–50], higher harmonics generation [51], or the spontaneous creation of electron-positron pairs from the vacuum as predicted by Schwinger [8].

ACKNOWLEDGMENTS

We thank M. Maggio, S. Norris, and A. Vikartofsky for help regarding the parallelization of the code. S.A. acknowledges the nice hospitality during his visit to ISU. This work has been supported by the NSF and the NSFC (Contract No. 11128409). It also used the Extreme Science and Engineering Discovery Environment (XSEDE), which is supported by NSF Grant No. OCI-1053575.

[1] See, e.g., S. S. Schweber, *An Introduction to Relativistic Quantum Field Theory* (Harper & Row, New York, 1962).
[2] I. Bialynicki-Birula and Z. Bialynicka-Birula, *Quantum Electrodynamics* (Pergamon Press, Oxford, 1975).
[3] W. Greiner, B. Müller, and J. Rafelski, *Quantum Electrodynamics of Strong Fields* (Springer Verlag, Berlin, 1985).
[4] R. H. Landau, *Quantum Mechanics II* (Wiley, New York, 1990).
[5] P. W. Miloni, *The Quantum Vacuum* (Academic Press, New York, 1993).
[6] See a review by I. P. Grant, in *Atomic, Molecular and Optical Physics*, edited by G. W. Drake (AIP Press, Woodbury, 1996).
[7] H. K. Avetissian, *Relativistic Nonlinear Electrodynamics* (Springer, New York, 2006).
[8] J. Schwinger, Phys. Rev. **82**, 664 (1951).
[9] B. Müller, H. Peitz, J. Rafelski, and W. Greiner, Phys. Rev. Lett. **28**, 1235 (1972).
[10] E. A. Uehling, Phys. Rev. **48**, 55 (1935).
[11] A. A. Grib, S. G. Mamayev, and V. M. Mostepanenko, *Quantum Effects in Intensive External Fields* (Atomizdat, Moscow, 1980), p. 296.
[12] A. Petermann and Y. Yamaguchi, Phys. Rev. Lett. **2**, 359 (1959).
[13] R. Glauber, W. Rarita, and P. Schwed, Phys. Rev. **120**, 609 (1960).
[14] For a recent review, see, e.g., A. Di Piazza, C. Müller, K. Z. Hatsagortsyan, and C. H. Keitel, Rev. Mod. Phys. **84**, 1177 (2012).
[15] B. Thaller, *The Dirac Equation* (Springer, Berlin, 1992).
[16] For a recent review, see, e.g., T. Cheng, Q. Su, and R. Grobe, Contemp. Phys. **51**, 315 (2010).
[17] J. A. Fleck, J. R. Morris, and M. D. Feit, Appl. Phys. **10**, 129 (1976).
[18] A. D. Bandrauk and H. Shen, J. Phys. A **27**, 7147 (1994).
[19] J. W. Braun, Q. Su, and R. Grobe, Phys. Rev. A **59**, 604 (1999).
[20] G. R. Mocken and C. H. Keitel, Comp. Phys. Commun. **178**, 868 (2008).
[21] M. Ruf, H. Bauke, and C. H. Keitel, J. Comp. Phys. **228**, 9092 (2009).
[22] P. Krekora, Q. Su, and R. Grobe, Phys. Rev. Lett. **92**, 040406 (2004).
[23] T. Cheng, S. P. Bowen, C. C. Gerry, Q. Su, and R. Grobe, Phys. Rev. A **77**, 032106 (2008).
[24] F. Sauter, Z. Phys. **69**, 742 (1931); **73**, 547 (1932).
[25] P. Krekora, Q. Su, and R. Grobe, Phys. Rev. Lett. **93**, 043004 (2004).
[26] T. Cheng, Q. Su, and R. Grobe, Las. Phys. **19**, 208 (2009).
[27] S. L. Haan, M. Dekker, E. Hamilton, and D. Streutker, Las. Phys. **9**, 190 (1999).
[28] C. C. Gerry, Q. Su, and R. Grobe, Phys. Rev. A **74**, 044103 (2006).
[29] P. Krekora, Q. Su, and R. Grobe, Phys. Rev. A **73**, 022114 (2006).
[30] F. Hebenstreit, J. Berges, and D. Gelfand, Phys. Rev. D **87**, 105006 (2013).
[31] F. Hebenstreit, J. Berges, and D. Gelfand, Phys. Rev. Lett. **111**, 201601 (2013).
[32] A. T. Steinacher, R. E. Wagner, Q. Su, and R. Grobe, Phys. Rev. A **89**, 032119 (2014).
[33] See several remarks in Ref. [3]. On page 4 it is pointed out that "charge density is positive nearer to the positive charge source," and on page 412 it reiterates that "the vacuum polarization actually strengthens the total potential generated by a (bare) charge density."
[34] S. Iso and H. Murayama, Prog. Theor. Phys. **84**, 142 (1990).
[35] Y.-Z. Chu and T. Vachaspati, Phys. Rev. D **81**, 085020 (2010).
[36] For a proposal for the development of the ELI program, see http://www.extreme-light-infrastructure.eu
[37] For work at the University of Texas at Austin, see http://www.ph.utexas.edu/~utlasers
[38] For work at Stanford, see https://slacportal.slac.stanford.edu/sites/lcls_public/
[39] For work at the University of Nebraska-Lincoln, see http://www.unl.edu/diocles/index.shtml
[40] For programs at GSI, see: http://www.gsi.de/fair/experiments/sparc
[41] See the European x-ray laser project XFEL homepage at http://xfel.desy.de/

[42] The Vulcan 10 Petawatt project: http://www.clf.rl.ac.uk/Facilities/Vulcan/12248.aspx
[43] For HiPER in England, see http://www.hiper-laser.org/. For Astra Gemini at RAL, see: http://www.clf.rl.ac.uk/Facilities/Astra/Astra+Gemini/12258.aspx
[44] http://www.physik.uni-jena.de/inst/polaris
[45] For work at the Chinese Academy of Sciences, see: http://highfield.iphy.ac.cn/
[46] For work at Shanghai Jiaotong University, see: http://ips.sjtu.edu.cn/
[47] M. Marklund and P. K. Shukla, Rev. Mod. Phys. **78**, 591 (2006).
[48] A. Di Piazza, K. Z. Hatsagortsyan, and C. H. Keitel, Phys. Rev. Lett. **97**, 083603 (2006).
[49] A. Di Piazza, A. I. Milstein, and C. H. Keitel, Phys. Rev. A **76**, 032103 (2007).
[50] A. Di Piazza and K. Z. Hatsagortsyan, Eur. Phys. J. **160**, 147 (2008).
[51] A. Di Piazza, K. Z. Hatsagortsyan, and C. H. Keitel, Phys. Rev. D **72**, 085005 (2005).